Electrical excitation of microcavity polaritons by radiative pumping from a weakly coupled organic semiconductor

Grant H. Lodden and Russell J. Holmes*
Department of Chemical Engineering and Materials Science, University of Minnesota, Minneapolis, Minnesota 55455, USA
(Received 13 August 2010; published 15 September 2010)

In an organic semiconductor, the population of microcavity polariton states occurs via an uncoupled exciton reservoir. Consequently, this results in the inefficient excitation of the upper polariton branch, and a significant population of uncoupled excitons in the active material. Here, an alternate excitation approach is demonstrated that permits the direct population of microcavity polariton states under both electrical and optical excitation without first forming an exciton reservoir. This is realized by introducing a weakly coupled emitter into an optical microcavity containing an organic semiconductor suitable for strong exciton-photon coupling. In contrast to previous work on microcavity polariton luminescence in organic semiconductors, angle-resolved measurements of the photoluminescence and electroluminescence show variations in upper and lower branch emission intensity consistent with the branch photon character. These results confirm that the excitation of the microcavity polariton states is by radiative pumping from the weakly coupled emitter.

DOI: 10.1103/PhysRevB.82.125317 PACS number(s): 71.36.+c, 42.50.Pq, 81.05.Fb, 71.35.Aa

I. INTRODUCTION

Organic semiconductors have received significant interest for application in optical microcavities in the regime of strong exciton-photon coupling.[1–3] The large exciton binding energies and oscillator strengths of these systems have enabled the observation of giant Rabi splittings ($\hbar\Omega > 100$ meV), permitting the study of strong coupling at room temperature under both optical and electrical excitation.[1,2,4–10] The regime of strong exciton-photon coupling is characterized by a reversible energy exchange between the resonant photon mode of the optical microcavity and the excitonic resonance of the semiconductor.[11] The strongly coupled system is characterized by new eigenstates known as microcavity polaritons. Experimentally, microcavity polaritons are identified by an energy-in-plane wave vector (or angle of detection) dispersion consisting of two branches that anticross at the point of energy degeneracy.[12] At the anticrossing point, the exciton-photon interaction is largest and the upper branch and lower branch are separated in energy by $\hbar\Omega$.[13]

While both inorganic and organic semiconductors have been used as the active medium in strongly coupled optical microcavities, their experimental behavior can be considerably different.[2–4,7–9,12,14–16] Provided that the upper and lower polariton branches are populated equally, the intensity of microcavity polariton luminescence is determined by the branch photon character. As a result, emission from the lower (upper) branch is expected to decrease (increase) in intensity with increasing detection angle, while at resonance, the emission intensity from both branches should be equal. The scaling of emission intensity with the photon character of the branch is frequently observed in inorganic semiconductor microcavities under low excitation powers.[12,15–17] In contrast, polariton luminescence from organic semiconductor microcavities does not reflect the variation in branch photon character with angle. In fact, emission from the upper branch is typically much smaller in intensity than that from the lower polariton branch for all angles of detection.[2,4,18]

Theoretical models have attempted to elucidate the mechanism for the population of the upper branch and identify the reason for its weak luminescence relative to the lower branch.[18–21] Typically, population of the upper branch is modeled as necessitating thermal activation from an uncoupled exciton reservoir.[19–21] The population of the upper branch is thus inefficient at room temperature, resulting in only weak emission relative to the lower branch. Since reservoir excitons may themselves undergo radiative or nonradiative decay prior to populating either the upper or lower branch, the intermediate population of the reservoir may constitute a potential loss channel, reducing the fraction of the pump excitation that results in microcavity polariton formation. Bimolecular quenching processes between reservoir excitons and microcavity polaritons have also been suggested as a potential pathway for additional loss.[22] In order to circumvent these complications, a microcavity architecture is demonstrated that permits the direct excitation of both the upper and lower polariton branches.

This paper is organized as follows. In Sec. II, the experimental details including device fabrication and various characterization techniques are described. The theoretical basis used to interpret the experimental results is developed in Sec. III while experimental results are presented in Sec. IV. A discussion of the results is provided in Sec. V, and the conclusions of this work are presented in Sec. VI.

II. EXPERIMENTAL

Optical microcavities were constructed by depositing organic and metallic layers onto a glass substrate coated with a 150-nm-thick layer of indium-tin-oxide (ITO) using vacuum thermal sublimation at 8×10^{-7} Torr. Prior to layer deposition, substrates were degreased with solvents and cleaned by exposure to UV-ozone ambient. The microcavity structure [Fig. 1(a)] consisted of a 50-nm-thick layer of Ag, a layer of tetraphenylporphyrin (TPP) of varying thickness, a 10-nm-thick layer of the hole-transporting material N,N′-bis(naphthalen-1-yl)-N,N′-bis(phenyl)-benzidine

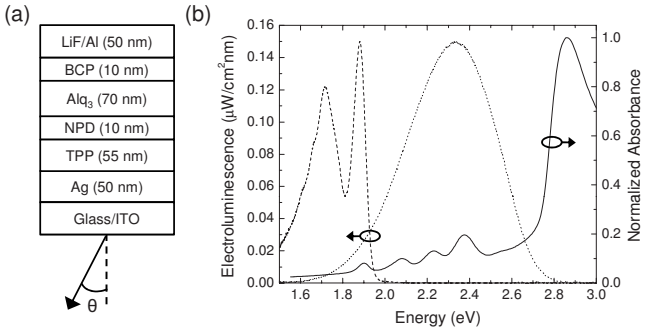

FIG. 1. (a) Microcavity architecture of interest for the study of radiative pumping. (b) Absorption (solid line) and electroluminescence (EL, dashed line) spectra of TPP and the electroluminescence (dotted line) of Alq_3. The EL spectra of TPP and Alq_3 were obtained in device architectures consisting of ITO/30 nm NPD/70 nm TPP or Alq_3/30 nm BCP/0.5 nm LiF/50 nm Al, respectively, at a current density of 100 mA/cm^2.

(NPD), a 70-nm-thick layer of the electron-transporting material aluminum tris(8-hydroxyquinoline) (Alq_3), and a 10-nm-thick layer of the exciton/hole-blocking material bathocuproine (BCP). The device cathode consisted of a 0.5-nm-thick layer of LiF and a 50-nm-thick layer of Al. The metallic anode (Ag) and cathode (Al) of the device also serve as reflectors forming an optical microcavity.[2,23] The layer of TPP serves as the active material for the observation of strong exciton-photon coupling.[24] Despite the proximity of TPP to the metallic anode, significant overlap with the optical field is maintained. The microcavity is tuned to resonance with the excitonic transition of TPP at (1.90 ± 0.02) eV [Fig. 1(b)]. The broad absorption and emission features of Alq_3 ensure only a weak coupling with the cavity photon mode.[25] The energy gap of the NPD layer is larger than that of Alq_3, preventing the direct excitation of TPP by blocking electrons and also preventing Förster energy transfer from Alq_3.[26] As such, devices constructed on ITO with no bottom reflector show electroluminescence (EL) only from Alq_3, confirming that there is no exciton formation on TPP. When excited, Alq_3 radiatively populates the polariton modes of the microcavity, circumventing the need to first create an uncoupled exciton reservoir. This excitation mechanism drastically alters the resulting EL and photoluminescence (PL) observed from the cavity.

Microcavities were characterized using a variety of angle-resolved techniques. Reflectivity measurements were performed using a variable-angle spectroscopic ellipsometer under *p*-polarized light illumination. A polarizer was used to collect *p*-polarized EL and PL spectra as a function of detection angle. For measurements of EL, devices were excited at a constant current density of 100 mA/cm^2. For measurements of PL, microcavities were excited using a 60 mW laser at a wavelength of $\lambda = 405$ nm. The laser was incident on the sample through the cathode in order to maximize the fraction of light absorbed in the Alq_3 layer.

III. THEORY

The use of radiative pumping permits equal population of the upper and lower polariton branches. When both polariton branches are populated equally, the emission intensity is dictated by the relative photon character of each branch. To assess the degree to which the observed emission features vary according to their relative photon character, the integrated EL intensities are related to the photon character using the following expression for emission from the lower (I^l) and upper (I^u) branches:[27]

$$I^{l,u} = \phi^{l,u} \frac{hcd_{Exc}}{\lambda^{l,u}} k_R^{l,u} N^{l,u}, \tag{1}$$

where the emission efficiency and wavelength are denoted as $\phi^{l,u}$ and $\lambda^{l,u}$, respectively. The polariton population and radiative decay rates of the lower and upper branches are denoted by $N^{l,u}$ and $k_R^{l,u}$, respectively. Under electrical excitation, the exciton recombination zone (d_{Exc}) in Alq_3 is approximated as the layer thickness.[28] The emission efficiency is taken as unity for both the upper and lower branches assuming that the radiative decay rate is much larger than the nonradiative decay rate for polaritons. The radiative decay rate of a polariton is related to the cavity photon lifetime (τ_{cav}) and the relative weight of the photon component of the polariton (α^2) by[18]

$$k_R^{u,l} \approx \frac{\alpha_{u,l}^2}{\tau_{cav}}. \tag{2}$$

Assuming that the lower and upper branches are populated equally, the relative weight of the photon component of the upper branch (α_u^2) can be written in terms of the EL intensity using Eq. (1) as

$$\alpha_u^2 = \frac{I^u \lambda^u}{I^l \lambda^l + I^u \lambda^u}. \tag{3}$$

An analogous expression for the lower branch (α_l^2) can also be derived.

IV. RESULTS

Figure 2(a) shows angle-resolved reflectivity spectra for a microcavity containing a (55 ± 2)-nm-thick layer of TPP. Two spectral features show strong dispersion with angle as a result of strong coupling between the cavity photon and the exciton resonance of TPP at 1.90 eV. A third feature observed at high energy results from coupling between the excitonic transition at 2.09 eV and the cavity mode. The dispersion relation of Fig. 2(b) was extracted from reflectivity and fit using a damped two-branch coupled-oscillator model having the cavity length, the effective refractive index and the cavity mode linewidth as adjustable parameters, and the Rabi splitting and exciton energy as fixed parameters.[29] A Rabi splitting of (74 ± 10) meV was determined from the minimum energetic separation between the upper and lower branches. A cavity length of (142 ± 10) nm, a refractive index of (2.39 ± 0.04), and a cavity mode linewidth of (65 ± 3) meV were obtained from the fit. The obtained cavity length is close to the total organic-layer thickness between the two electrodes.

Figures 3(a) and 3(b) show angle-resolved EL and PL spectra, respectively, for a device containing a

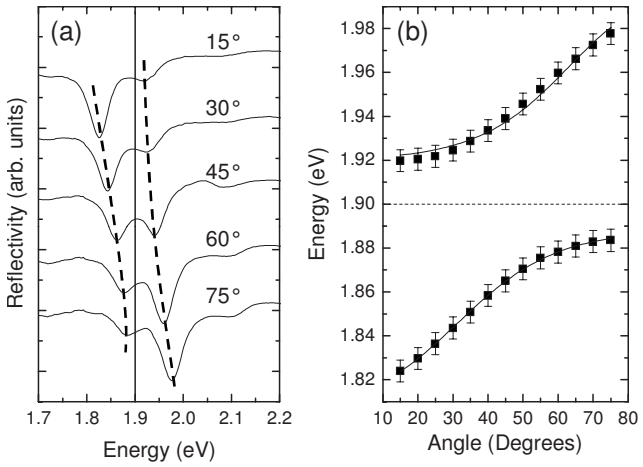

FIG. 2. (a) Reflectivity spectra for the microcavity of Fig. 1(a). Broken lines highlight the dispersion of the lower and upper branch polariton features with angle. (b) Dispersion relation obtained from angle-resolved reflectivity measurements for the microcavity of (a). Solid lines are damped coupled-oscillator fits while the broken line indicates the position of the uncoupled excitonic transition of TPP.

(55 ± 2)-nm-thick layer of TPP. As in reflectivity, two emission features exhibiting strong dispersion are observed as a result of coupling between the excitonic transition at 1.90 eV and the cavity photon. The additional feature observed at high energy again results from strong coupling between the cavity photon and the excitonic transition at 2.09 eV. Under electrical pumping, the intensity of the polariton features shows dispersion with angle that reflects their photon character [Fig. 3(a)]. Emission from the two branches is nearly equal in intensity at ~45°, consistent with the reflectivity spectra of Fig. 2(a). For measurements of PL [Fig. 3(b)], emission from the upper and lower branches is not equal in intensity at 45°. Here, the lower branch has additional weight due to direct optical pumping of TPP in addition to radiative pumping via Alq_3. The absorption coefficients for TPP, NPD, and Alq_3 at 405 nm were separately measured by ellipsometry to be 3.6×10^5 cm^{-1}, 2.6×10^4 cm^{-1}, and 3.1×10^4 cm^{-1}, respectively. As such, additional population of the exciton reservoir of TPP may occur via Förster energy transfer from NPD under optical pumping. Consequently, the electrically pumped structure is better suited to examine radiative pumping of TPP since it permits the excitation to be localized to Alq_3. Nevertheless, intense emission from the upper branch is clearly observed under optical excitation as a result of radiative pumping from Alq_3.

The dispersion relations shown in Fig. 3(c) were constructed by using multipeak fitting to extract peak centers from the spectra of Figs. 3(a) and 3(b). Both the EL and PL dispersion relations were fit with a damped two-branch coupled-oscillator model. A Rabi splitting of (85 ± 5) meV was extracted from the energy difference between the upper and lower branches. The fit shown in Fig. 3(c) corresponds to a cavity length of (143 ± 10) nm, a refractive index of (2.36 ± 0.09), and a cavity mode linewidth of (76 ± 5) meV.

V. DISCUSSION

Figures 4(a) and 4(b) show microcavity EL and PL for devices where the coupling medium (TPP) is excited either

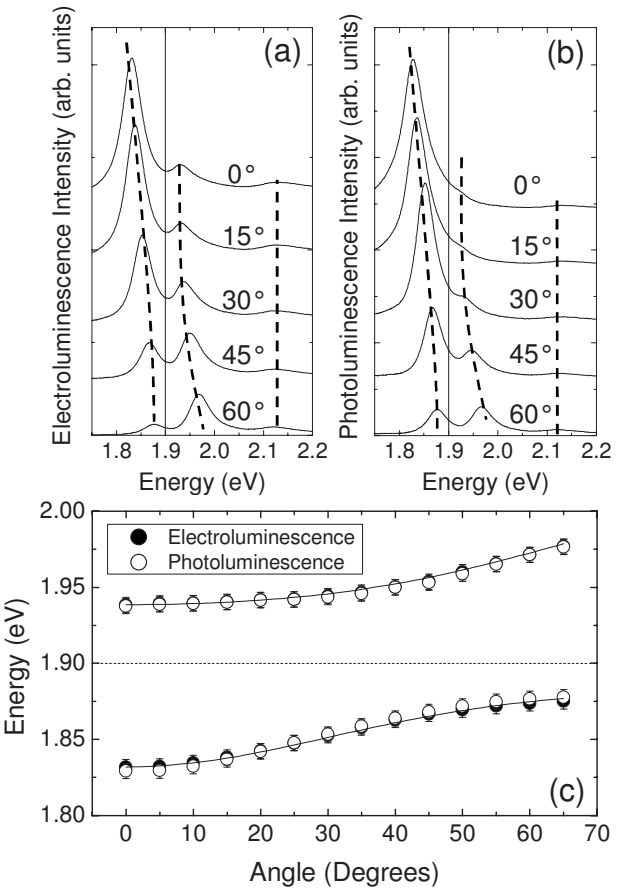

FIG. 3. Angle-resolved (a) EL and (b) PL for the microcavity of Fig. 1(a). Solid lines denote the position of the uncoupled excitonic transition of TPP while the broken lines highlight the dispersion of strongly coupled features with angle. (c) Dispersion relations extracted from angle-resolved measurements of EL and PL. The solid line is a damped coupled-oscillator fit. The position of the TPP excitonic transition is indicated by the broken line.

by radiative pumping from Alq_3 or from the TPP exciton reservoir. The microcavity architecture used for the radiative pumping of TPP is shown in Fig. 1 while the microcavity used to study the pumping of TPP via the exciton reservoir consisted of a 50-nm-thick Ag anode, a 30-nm-thick layer of NPD, a 70-nm-thick layer of TPP, and a 30-nm-thick layer of BCP. The cathode consisted of a 5-nm-thick layer of LiF and a 50-nm-thick layer of Al. In the latter structure, electrical or optical excitation leads to exciton formation in TPP. Layer thicknesses were chosen to ensure a similar exciton-photon detuning for both structures. The pumping of TPP from the exciton reservoir [Figs. 4(a) and 4(b), broken line] results mainly in the observation of lower branch emission with only weak luminescence from the upper branch. When the TPP active layer is radiatively pumped [Figs. 4(a) and 4(b), solid line], luminescence from Alq_3 is absorbed by the microcavity polariton resonances.[24] This results in intense luminescence from both the upper and lower polariton branches without first populating the exciton reservoir.[21] Due to the low-cavity quality factor ($Q \sim 28$), weak uncoupled emission from Alq_3 is also observed with depressions in the spectra corresponding to absorption by the excitonic transi-

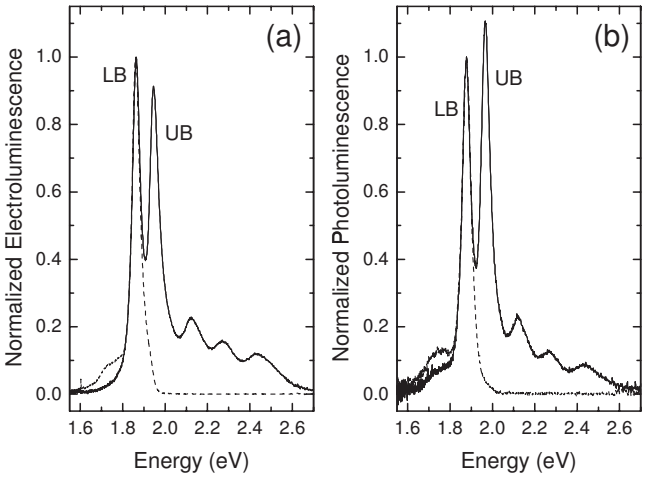

FIG. 4. Normalized (a) EL and (b) PL for microcavities where the TPP active layer is excited either via the exciton reservoir (broken line) or by radiative pumping (solid line). The spectra are for microcavities with similar detunings. Microcavity polariton luminescence is identified as originating from either the lower branch (LB) or upper branch (UB).

tions of TPP at 2.22 and 2.38 eV.[18] No uncoupled emission is observed from TPP, suggesting that only polariton states are populated in the active layer.

As discussed in Sec. III, the degree to which the observed emission features vary according to their relative photon character can be assessed using Eq. (3). The values obtained for the relative weight of the photon component from EL can be compared directly to the branch photon character extracted from the dispersion relation of Fig. 3(c).[13] Figure 5 shows the result of this comparison for a microcavity containing 55 nm of TPP. The photon fraction derived from the peak EL intensities shows good agreement with the actual photon character obtained from the EL dispersion, confirming that radiative pumping of microcavity polariton states circumvents any barrier for the population of the upper branch.

In many inorganic semiconductors, charge transport in the active coupling layer is problematic due to the potential for exciton screening and dissociation.[16,30] In order to radiatively pump such structures using the architecture discussed here, a thin, semitransparent metal electrode could be included above the active layer to electrically pump the weakly coupled emitter. In this way, there is no charge transport through the active layer for strong coupling and the excitation of polariton modes is exclusively by radiative pumping.

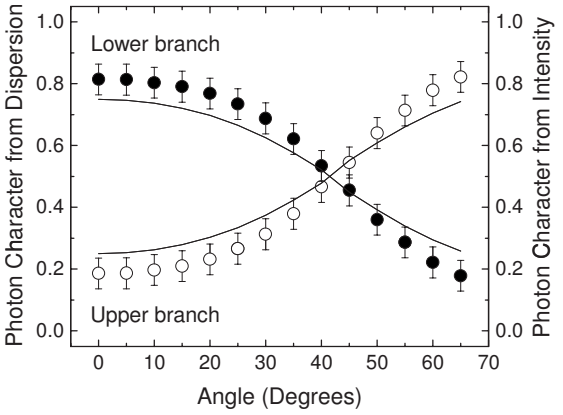

FIG. 5. Photon character of the upper and lower polariton branches derived from the EL dispersion relation of Fig. 3(c) (solid lines) and the EL intensity of Fig. 3(a) using Eq. (3) (circles). The lower and upper branches are denoted by filled and open circles, respectively.

This use of radiative pumping may ultimately facilitate the electrical excitation of polariton modes in inorganic semiconductors characterized by a small exciton binding energy.

VI. CONCLUSION

A microcavity architecture is demonstrated that permits the direct population of polariton states in an organic semiconductor, eliminating the need to first form an uncoupled exciton reservoir. Microcavity polaritons in this structure are radiatively pumped by a weakly coupled emissive layer under electrical or optical excitation. Luminescence originates from microcavity polariton modes and reflects the photon character of the upper and lower branches. The use of radiative pumping offers an alternate excitation scheme for the realization of polariton-based optoelectronic devices. This excitation approach may serve as a platform through which to study polariton states which are typically not populated due to rapid exciton relaxation to lower energy, nonradiative states.[5,24,31–33]

ACKNOWLEDGMENTS

Primary support for this work was received from the University of Minnesota Industrial Partnership for Research in Materials and Interfacial Engineering. Partial support was also received from the NSF MRSEC Program under Award No. DMR-0819885. Part of this work was carried out in the Institute of Technology Characterization Facility, University of Minnesota, which has received funding from NSF through the MRSEC, ERC, and MRI programs.

*rholmes@umn.edu

[1] D. G. Lidzey, D. D. C. Bradley, M. S. Skolnick, T. Virgili, S. Walker, and D. M. Whittaker, Nature (London) **395**, 53 (1998).

[2] J. R. Tischler, M. S. Bradley, V. Bulovic, J. H. Song, and A. Nurmikko, Phys. Rev. Lett. **95**, 036401 (2005).

[3] R. J. Holmes and S. R. Forrest, Org. Electron. **8**, 77 (2007).

[4] D. G. Lidzey, D. D. C. Bradley, T. Virgili, A. Armitage, M. S. Skolnick, and S. Walker, Phys. Rev. Lett. **82**, 3316 (1999).

[5] D. G. Lidzey, D. D. C. Bradley, A. Armitage, S. Walker, and M. S. Skolnick, Science **288**, 1620 (2000).

[6] S. Kéna-Cohen, M. Davanço, and S. R. Forrest, Phys. Rev. Lett.

101, 116401 (2008).
[7] N. Takada, T. Kamata, and D. D. C. Bradley, Appl. Phys. Lett. **82**, 1812 (2003).
[8] R. J. Holmes and S. R. Forrest, Phys. Rev. Lett. **93**, 186404 (2004).
[9] P. Schouwink, H. V. Berlepsch, L. Dahne, and R. F. Mahrt, Chem. Phys. Lett. **344**, 352 (2001).
[10] P. Schouwink, H. von Berlepsch, L. Dahne, and R. F. Mahrt, Chem. Phys. **285**, 113 (2002).
[11] C. Weisbuch, M. Nishioka, A. Ishikawa, and Y. Arakawa, Phys. Rev. Lett. **69**, 3314 (1992).
[12] R. Houdré, C. Weisbuch, R. P. Stanley, U. Oesterle, P. Pellandini, and M. Ilegems, Phys. Rev. Lett. **73**, 2043 (1994).
[13] M. S. Skolnick, T. A. Fisher, and D. M. Whittaker, Semicond. Sci. Technol. **13**, 645 (1998).
[14] G. Christmann, R. Butté, E. Feltin, A. Mouti, P. A. Stadelmann, A. Castiglia, J. F. Carlin, and N. Grandjean, Phys. Rev. B **77**, 085310 (2008).
[15] A. I. Tartakovskii, V. D. Kulakovskii, A. V. Larionov, J. P. Reithmaier, and A. Forchel, Phys. Status Solidi A **164**, 81 (1997).
[16] S. I. Tsintzos, N. T. Pelekanos, G. Konstantinidis, Z. Hatzopoulos, and P. G. Savvidis, Nature (London) **453**, 372 (2008).
[17] R. P. Stanley, R. Houdré, C. Weisbuch, U. Oesterle, and M. Ilegems, Phys. Rev. B **53**, 10995 (1996).
[18] D. G. Lidzey, A. M. Fox, M. D. Rahn, M. S. Skolnick, V. M. Agranovich, and S. Walker, Phys. Rev. B **65**, 195312 (2002).
[19] P. Michetti and G. C. La Rocca, Phys. Rev. B **79**, 035325 (2009).
[20] P. Michetti and G. C. La Rocca, Phys. Rev. B **77**, 195301 (2008).
[21] S. Ceccarelli, J. Wenus, M. S. Skolnick, and D. G. Lidzey, Superlattices Microstruct. **41**, 289 (2007).
[22] M. Litinskaya, P. Reineker, and V. M. Agranovich, J. Lumin. **119-120**, 277 (2006).
[23] P. A. Hobson, W. L. Barnes, D. G. Lidzey, G. A. Gehring, D. M. Whittaker, M. S. Skolnick, and S. Walker, Appl. Phys. Lett. **81**, 3519 (2002).
[24] R. J. Holmes and S. R. Forrest, Phys. Rev. B **71**, 235203 (2005).
[25] A. Dodabalapur, L. J. Rothberg, R. H. Jordan, T. M. Miller, R. E. Slusher, and J. M. Phillips, J. Appl. Phys. **80**, 6954 (1996).
[26] I. G. Hill, A. Kahn, J. Cornil, D. A. dos Santos, and J. L. Bredas, Chem. Phys. Lett. **317**, 444 (2000).
[27] A. Yariv, *Optical Electronics in Modern Communications* (Oxford University Press, New York, 1997).
[28] J. Kalinowski, L. C. Palilis, W. H. Kim, and Z. H. Kafafi, J. Appl. Phys. **94**, 7764 (2003).
[29] V. Savona, L. C. Andreani, P. Schwendimann, and A. Quattropani, Solid State Commun. **93**, 733 (1995).
[30] R. Butté, G. Delalleau, A. I. Tartakovskii, M. S. Skolnick, V. N. Astratov, J. J. Baumberg, G. Malpuech, A. Di Carlo, A. V. Kavokin, and J. S. Roberts, Phys. Rev. B **65**, 205310 (2002).
[31] S. Kéna-Cohen and S. R. Forrest, Phys. Rev. B **76**, 075202 (2007).
[32] D. G. Lidzey, J. Wenus, D. M. Whittaker, G. Itskos, P. N. Stavrinou, D. D. C. Bradley, and R. Murray, J. Lumin. **110**, 347 (2004).
[33] R. J. Holmes, S. Kéna-Cohen, V. M. Menon, and S. R. Forrest, Phys. Rev. B **74**, 235211 (2006).